HHS Public Access

Author manuscript

Atherosclerosis. Author manuscript; available in PMC 2018 February 01.

Published in final edited form as:

Atherosclerosis. 2017 February ; 257: 38–46. doi:10.1016/j.atherosclerosis.2016.12.014.

The $P2Y_2$ nucleotide receptor is an inhibitor of vascular calcification

Shaomin Qian[1], **Jenna N. Regan**[2], **Maxwell T. Shelton**[1], **April Hoggatt**[1], **Khalid S. Mohammad**[2], **Paul B. Herring**[1], and **Cheikh I. Seye**[1,*]

[1]Cellular & Integrative Physiology, Indiana University School of Medicine, Indianapolis, IN, USA

[2]Medicine/Endocrinology, Indiana University School of Medicine, Indianapolis, IN, USA

Abstract

Background and aims—Mutations in the 5′-nucleotidase ecto *(NT5E)* gene that encodes CD73, a nucleotidase that converts AMP to adenosine, are linked to arterial calcification. However, the role of purinergic receptor signaling in the pathology of intimal calcification is not well understood. In this study, we examined whether extracellular nucleotides acting via $P2Y_2$ receptor ($P2Y_2R$) modulate arterial intimal calcification, a condition highly correlated with cardiovascular morbidity.

Methods—Apolipoprotein E, $P2Y_2R$ double knockout mice ($ApoE^{-/-}P2Y_2R^{-/-}$) were used to determine the effect of $P2Y_2R$ deficiency on vascular calcification *in vivo*. Vascular smooth muscle cells (VSMC) isolated from $P2Y_2R^{-/-}$ mice grown in high phosphate medium were used to assess the role of $P2Y_2R$ in the conversion of VSMC into osteoblasts. Luciferase-reporter assays were used to assess the effect of $P2Y_2R$ on the transcriptional activity of Runx2.

Results—$P2Y_2R$ deficiency in $ApoE^{-/-}$ mice caused extensive intimal calcification despite a significant reduction in atherosclerosis and macrophage plaque content. The ectoenzyme apyrase that degrades nucleoside di- and triphosphates accelerated high phosphate-induced calcium deposition in cultured VSMC. Expression of $P2Y_2R$ inhibits calcification *in vitro* inhibited the osteoblastic trans-differentiation of VSMC. Mechanistically, expression of $P2Y_2R$ inhibited Runx2 transcriptional activation of an osteocalcin promoter driven luciferase reporter gene.

Conclusions—This study reveals a role for vascular $P2Y_2R$ as an inhibitor of arterial intimal calcification and provides a new mechanistic insight into the regulation of the osteoblastic trans-differentiation of SMC through $P2Y_2R$-mediated Runx2 antagonism. Given that calcification of atherosclerotic lesions is a significant clinical problem, activating $P2Y_2R$ may be an effective therapeutic approach for treatment or prevention of vascular calcification.

*Corresponding author: Department of Cellular & Integrative Physiology, Indiana University School of Medicine 635 Barnhill Drive MS 332, Indianapolis, IN 46202. cseye@iu.edu (C. Seye).

Conflict of interest

The authors declared they do not have anything to disclose regarding conflict of interest with respect to this manuscript.

Keywords

ATP; Atherosclerosis; Nucleotide receptor; Vascular calcification; Inflammation

Introduction

Vascular calcification is a hallmark of many diseases including atherosclerosis, type 2 diabetes, end-stage renal disease, and is highly correlated with cardiovascular morbidity (1–2). Arterial medial calcification occurs in the absence of inflammation, and is associated with chronic kidney disease (CDK) in adults (3–5). Medial calcification causes vessel stiffening, elevated pulse-wave velocity, and increased left ventricular (LV) load with hypertrophy (6–9). In contrast, intimal calcification occurs in the context of atherosclerosis and is associated with plaque rupture and myocardial infarction (10–12). Vascular calcification is an active and regulated process reminiscent of physiological bone formation (12). VSMC are the main cell type involved in arterial calcification, and can trans-differentiate into an osteoblast-like cell (13–14). This phenotypic transition is characterized by the expression of alkaline phosphatase, type I collagen, osteocalcin and the formation of mineralized bone-like structures (15).

Runt-related transcription factor (Runx) 2 is a key regulator of osteoblast differentiation (16). Runx2-null mice are devoid of osteoblasts and lack the ability to form bone (17–18). Runx2 mediates osteoblast differentiation as well as mineralization in immature mesenchymal cells and osteoblastic cells *in vitro* (19–20). Runx2 is expressed in calcified human atherosclerotic lesions as well as in calcifying mouse aortic SMC (21–23). Expression of Runx2 alone does not induce VSMC calcification *in vitro* (24), however, Runx2 deficiency in VSMC has been shown to inhibit vascular calcification *in vivo* (25). Given the pivotal role of Runx2 in SMC calcification, identifying factors that regulate this transcription factor may lead to new medical therapies to prevent or treat cardiovascular calcification.

A study of idiopathic infantile arterial calcification first led to the hypothesis that the purinergic signaling may play a role in the pathogenesis of vascular calcification (26). This autosomal recessive disease is caused by a mutation in the ectonucleotide pyrophosphatase-phosphodiesterase 1 gene (*ENPP1*) that catalyzes the hydrolysis of pyrophosphate and phosphodiester bonds in nucleotide triphosphates and oligonucleotides, respectively, to generate nucleoside 5′-monophosphates. In addition, homozygous nonsense mutations in the 5′-nucleotidase ecto *(NT5E)* gene that encodes *CD73*, a nucleotidase that converts AMP to adenosine, have been linked to symptomatic arterial and joint calcifications (27). Together, these observations suggest a role for the AMP/adenosine metabolic pathway in inhibiting ectopic tissue calcification. Indeed, increased cAMP signaling synergizes with elevated extracellular inorganic phosphate (P_i) to induce calcification of vascular SMC (28). However, the role of purinergic receptor signaling in the pathogenesis of vascular calcification, particularly in the setting of atherosclerosis, is not understood.

The $P2Y_2$ is expressed in vascular cells and its activation mediates inflammatory responses that contribute to intimal hyperplasia in response to injury (29–31). We recently showed that

$P2Y_2R$ deletion prevents fatty-streaks formation in ApoE-null mice (32). In the present study, we examined the effects of $P2Y_2R$ deletion on arterial intimal calcification during atherosclerosis. We utilized the ApoE knockout mouse model of atherosclerosis which develops spontaneous atherosclerosis without dietary manipulations (33). By crossing ApoE knockout mice with $P2Y_2R$ knockout mice, we show that although loss of $P2Y_2R$ attenuates atherosclerotic plaque development, it leads to extensive calcification of the atherosclerotic lesions. *In vitro*, high Pi induced-calcium deposition in VSMC and expression of stage-specific osteoblast markers were exacerbated in the absence of $P2Y_2R$. Finally, we demonstrated that $P2Y_2R$ prevents the osteoblastic trans-differentiation of VSMC by inhibiting Runx2 transcriptional activity. Our findings reveal a novel role of $P2Y_2R$ in the control of vascular calcification. Therefore, targeting $P2Y_2R$ signals in VSMC may represent a novel strategy for therapies targeting vascular calcification.

Materials and methods

Animals

Animal protocols were approved by the Animal Care and Use Committee of Indiana University and the procedures followed were in accordance with institutional guidelines. C57BL/6J, $ApoE^{-/-}$ and $P2Y_2R^{-/-}$ mice were purchased from Jackson laboratory. $P2Y_2R^{-/-}$ mice were bred to the $ApoE^{-/-}$ background to generate $ApoE^{-/-}/P2Y_2R^{-/-}$ mice. All of these mice are on a C57BL/6J background. All animals were fed a standard chow diet. Only males were used in experimental groups.

Analysis of atherosclerotic lesions in the aortic root

Mouse hearts were perfused, fixed in 4% paraformaldehyde and embedded in paraffin. Five-micrometer sections at 50-μm intervals were stained with Masson's trichrome for lesion area measurement and morphometric analysis as described in our previous studies (32). Apoptosis was assessed by TUNEL (Tdt-mediated dUTP nick end labeling) method using the TACS 2 TdT *in situ* apoptosis detection kit (Trevigen). For the quantification of plaque necrosis, aortic root lesions were stained with hematoxylin/eosin. Necrotic areas were identified as large non-stained areas with a 3,000-μm^2 threshold, thus excluding very small clear areas, and quantified as previously described (34).

In situ detection of calcification

Intimal calcification was detected by performing Von Kossa staining on tissue sections. Von Kossa-stained sections were then counterstained for hematoxylin and eosin. Von Kossa reactivity was quantified and expressed as a percentage of Von Kossa positive area divided by total lesion area.

Tissue and cell quantification of calcium

Aortic arch specimens from mice were lyophilized to a constant weight. The calcium extracted from lyophilized tissue with 0.6 N HCl at 37°C for 48 hours was measured by a colorimetric assay using the o-cresolphsthalein complexone kit (calcium diagnostic kit; Sigma-Aldrich). The amount of calcium was normalized to the tissue dry weight. Calcium content in cultured VSMC was determined using a similar procedure as described above,

and expressed as micrograms of calcium per milligram of cellular protein. Protein content was measured using the bicinchoninic acid assay protein assay kit (Thermo Scientific).

Immunohistochemistry

Immunohistochemical staining was performed by the labeled streptavidin biotin method. Monoclonal anti-smooth muscle α-actin antibody (clone 1A4, Sigma, 1/1000 dilution) was used to detect smooth muscle cells. Macrophages were identified by immunostaining with a rat anti-mouse Mac-3 monoclonal antibody (M3/84, 550292, BD PharMingen, San Diego, CA; 1/100 dilution).

VSMC calcification assay

Aortic samples were collected from C57BL/6 and $P2Y_2R^{-/-}$ mice and VSMC were isolated using the explant technique as described in our previous studies (34). SMC were seeded in growth medium at a density of $1.5 \times 10^4/cm^2$ in multi-well plates. Cells were grown to confluence and incubated with calcification medium containing NaH_2PO_4 and Na_2HPO_4 at pH 7, to a final concentration of 3 mM phosphate. VSMC were incubated for up to 14 days in 95% air/5% CO_2 and medium was changed every four days. Retroviral transduction of DNA construct into VSMC was performed as described in our previous studies (35).

Alizarin Red S staining

Cells were incubated in 10%-PFA for 10 minutes then rinsed with distilled water and dehydrated to 70% alcohol. Cells were stained with 2% Alizarin Red S solution for 5 minutes then blotted dry. The slides were then dehydrated in acetone and 1:1 acetone-xylene solution, cleared in xylene, and mounted using a synthetic mounting medium.

Luciferase reporter assays

Cells were transfected with firefly luciferase reporter 6×OSE2-Luc plus *Renilla* luciferase reporter pRL-TK. At 48 hours after transfection, cells were harvested and firefly and *Renilla* luciferase activities in cell lysates were measured using a dual luciferase kit (Promega). *Renilla* luciferase activities in cells were used as internal control.

Gene expression analysis

Quantitative polymerase chain reaction (qPCR) was performed as previously described (36). Total RNA was extracted from VSMC lysed in TRIzol reagent (Invitrogen), using an RNeasy mini kit and treated with DNase I (Qiagen). High quality RNA was extracted (0.5 μg/sample was used for synthesis of single-strand cDNA with Superscript II (Invitrogen). Syber green based real time PCR was conducted with 45 ng of cDNA using an ABI Prism 7900HT PCR machine (Applied Biosystems). The following primers (Integrated DNA Technologies) were used for *Runx2*: forward 5′-ACC ATA ACA GTC TTC ACA AAT CCT-3′, and reverse: 5′-CAG GCG ATC AGA GAA CAA ACT A-3′. The primers for *osteocalcin* were as follows: forward 5′-CTGACCTCACAGATGCCAAG-3′, and reverse: 5′-GTAGCGCCGGAGTCTGTTC-3′. *GAPDH* primers were used as internal control. The forward *GAPDH* primer was: 5′-GGT GGC AGA GGC CTT TG-3′. The reverse *GAPDH* primer was: 5′-TGC CCA TTT AGC ATC TCC TT-3′.

Statistical analysis

Data are expressed as means ± SEM. Differences in data between groups were compared with Student's paired 2-tailed t test or 1-way ANOVA where appropriate. A p value less than 0.05 was considered statistically significant.

Results

$P2Y_2$ receptor deficiency promotes calcification of atherosclerotic lesions

We assessed the effects of $P2Y_2R$ deletion on arterial calcification in $ApoE^{-/-}$ mice maintained on a standard mouse chow diet for 30 weeks. Strikingly, despite a significant decrease in atherosclerotic lesion area compared to $ApoE^{-/-}$ mice ($p<0.01$; Fig. 1A and B), $ApoE^{-/-}/P2Y_2R^{-/-}$ mice (15 out of 15 mice) exhibited extensive intimal calcification covering more than 10% of the plaque area ($p<0.001$; Fig. 1C–E). Micro-calcification in the form of spotty or granular calcium deposits was also observed in $ApoE^{-/-}/P2Y_2R^{-/-}$ mice (Fig. 1C). In contrast, large areas of calcification were absent from $ApoE^{-/-}$ lesions (Fig. 1C), and only 1 out of 15 $ApoE^{-/-}$ mice exhibited very few granular calcium deposits. Notably, no calcification was observed in the media layer in either genotype. Fig. 1C shows a typical lesion in the aortic root, with extensive calcification in close proximity of the endothelium. The amount of extractable calcium that was deposited in the aortic root in $P2Y_2R^{-/-}/ApoE^{-/-}$ mice was 10-fold greater compared to that of $ApoE^{-/-}$ mice (Fig. 1D). The calcified area occupied about 13% of the total lesion area (Fig. 1E). Vascular calcification observed in $P2Y_2R^{-/-}/ApoE^{-/-}$ mice was not due to an increase in plasma cholesterol since $P2Y_2R$-deficiency did not alter total plasma cholesterol in $ApoE^{-/-}$ mice (Table 1). These data demonstrate that absence of $P2Y_2R$ result in early calcification of atherosclerotic lesions in $ApoE^{-/-}$ mice.

$P2Y_2R$ deficiency reduces plaque cellularity

$P2Y_2R$ deficiency led to other differences in intimal plaque composition as well. The increased intimal calcification attributable to the loss of the $P2Y_2R$ gene correlated with a sharp reduction in the total plaque area occupied by Mac-3 positive macrophages ($p<0.001$, Fig. 2A) and a significant decrease in SMC content ($p<0.001$; Fig. 2B). Consequently, plaque cellularity (Fig. 3A) was decreased in lesions observed in $P2Y_2R^{-/-}/ApoE^{-/-}$ mice. Analysis of lesions for acellular/necrotic areas revealed a significant increase in plaque necrosis in the $ApoE^{-/-}/P2Y_2R^{-/-}$ lesions ($p<0.001$; Fig. 3B). We next examined if the increased necrosis in $ApoE^{-/-}/P2Y_2R^{-/-}$ lesions was due to an increase in cell apoptosis. As shown in Fig. 3C, apoptosis as measured by TUNEL-positive cells was 40% ($p<0.001$) higher in the $ApoE^{-/-}/P2Y_2R^{-/-}$ lesions. The formation of plaques with large necrotic/apoptotic cores is followed by conversion to highly fibrotic nodules, and many of the cells within the nodules express markers of chondrocytes and osteoblasts (37). Notably, cells within the calcified areas in the $ApoE^{-/-}/P2Y_2R^{-/-}$ lesions exhibited chondrocyte appearance and features such as abundant collagen fibers and proteoglycans reacting with the hematoxylin counterstaining (Fig. 3D),

Expression of $P2Y_2$ receptor inhibits VSMC calcification *in vitro*

As described previously by others (38), we confirmed that high P_i induces a significant increase in VSMC calcium deposition, evident after 14 days in culture as compared to cells cultured in control medium (Fig. 4A). Notably, adding an enzyme that degrades nucleoside di- and triphosphates (potato apyrase grade III, 0.1 unit/ml) greatly accelerated SMC calcification such that high levels of calcium content were measurable by 7 days of culture (Fig. 4B), suggesting that nucleotides released by VSMC inhibit calcification. $P2Y_2R$ deficiency in VSMC significantly increased high Pi-induced calcification as demonstrated by a sharp increase in the amount of incorporated calcium ($p<0.001$) compared to VSMC from WT mice (Fig. 5A; $p<0.001$) after 7 days of culture. Interestingly, the extent of calcification in $P2Y_2^{-/-}$ SMC was similar to cultures lacking nucleoside di- and triphosphates (Fig. 5A compared to Fig. 4B).

$P2Y_2$ receptor inhibits the osteogenic trans-differentiation of VSMC

Calcifying VSMC adopt an osteoblast-like phenotype, including expression of osteoblast markers (25). Therefore, we measured the expression of the stage-specific osteoblast markers Runx2 and osteocalcin in VSMC from WT or $P2Y_2R^{-/-}$ mice cultured in high Pi medium (Fig. 5B). Both osteoblast markers were expressed at significantly higher levels in $P2Y_2R^{-/-}$ VSMC, suggesting that the absence of $P2Y_2R$ sensitizes them to calcification promoting conditions. Conversely, rescue of $P2Y_2R$ expression in knockout VSMC (via retroviral transduction of full-length WT mouse $P2Y_2R$ into $P2Y_2R^{-/-}$ cells) decreased osteoblast-specific gene expression and total calcium content to levels comparable with WT (Fig. 5C and D). These results demonstrate that $P2Y_2R$ in VSMC is required to inhibit osteogenic trans-differentiation.

$P2Y_2$ receptor represses Runx2 transcriptional activity

As Runx2 is known to be required for VSMC calcification *in vitro* and *in vivo* (25, 39) and its expression was increased in $P2Y_2R^{-/-}$ VSMC, we examined whether expression of $P2Y_2R$ inhibits the transcriptional activity of Runx2. Overexpression of Runx2 increased the activity of an OC promoter driven luciferase reporter gene (40) in $P2Y_2R$-deficient VSMC (Fig. 6). However, this Runx2-induced OC promoter activity was significantly attenuated in $P2Y_2R$-deficient VSMC transduced with WT $P2Y_2R$ (Fig. 6). These data clearly indicate that $P2Y_2R$ regulates the osteogenic trans-differentiation of VSMC through Runx2 antagonism.

Discussion

The main finding of this study supports a dual role for $P2Y_2$ receptor as a mediator of atherosclerosis but an inhibitor of arterial intimal calcification. $P2Y_2R$ deficiency leads to reduced atherosclerotic lesion sizes, increased plaque necrosis with extensive calcification. Furthermore, loss of $P2Y_2R$ accelerates *in vitro* calcification and the osteoblastic trans-differentiation of VSMC. Mechanistically, $P2Y_2R$ acts as a negative regulator of Runx2 transcriptional activity.

Intimal calcification is apparent in normal chow fed *ApoE*$^{-/-}$ mice at around 45 weeks of age, where small deposits of hydroxyapatite are observed (37). Surprisingly, calcium deposits are apparent in *ApoE*$^{-/-}$/*P2Y*$_2$*R*$^{-/-}$ mice at high frequency, as early as 30 weeks of age, indicating that absence P2Y$_2$R accelerates intimal calcification. The calcified lesions were associated with decrease cellularity that is associated with a significant reduction in both macrophage and VSMC content of the plaques. The decrease in lesion cellularity observed in *ApoE*$^{-/-}$/*P2Y*$_2$*R*$^{-/-}$ mice was in part due to increased cell apoptosis.

Several factors may account for the increased calcification of the lesions in the *ApoE*$^{-/-}$ mice in the absence of P2Y$_2$R. Increased circulating LDL and decreased HDL have been shown to increase plaque burden and coronary artery calcification (42). However, since P2Y$_2$R deficiency does not alter plasma lipid content in the *ApoE*$^{-/-}$ mice (Table 1), this mechanism likely does not account for the increased calcification in these mice. The observation of bone-like regions within the lesions in *P2Y*$_2$*R*$^{-/-}$/*ApoE*$^{-/-}$ mice suggests that lack of P2Y$_2$R stimulates an active process similar to bone formation in the lesions.

Depending on the type of calcium deposition, intimal calcification may either promote the formation of rupture-prone lesions or stabilize the plaque (43). Our data indicate that P2Y$_2$R-deficiency drives the formation of both spotty calcium deposits (micro-calcification) and large calcified areas (macro-calcification). Micro-calcification which induces further inflammation is associated with unstable plaques while macro-calcification favors plaque stabilization (43). It is possible that the large areas of calcium deposits in lesions from *ApoE*$^{-/-}$/*P2Y*$_2$*R*$^{-/-}$ mice represent an adaptive mechanism to counter the initial detrimental effects caused by small granular calcium deposits. The increased stability associated with large calcium deposits would be consistent with increased plaque stability resulting from the significantly reduced macrophage content in lesions from *ApoE*$^{-/-}$/*P2Y*$_2$*R*$^{-/-}$ mice. This reduction in plaque macrophage content was also correlated with the presence of chondrocyte-like cells that are often seen in stabilized plaques (37).

Osteogenic trans-differentiation of VSMC is known to contribute directly to the pathogenesis of atherosclerotic calcification (25). Our data show that extracellular nucleotides act as inhibitors of VSMC calcification *in vitro*. Indeed, the enzyme potato apyrase that degrades nucleoside di- and triphosphates accelerated VSMC calcification under an osteogenic environment. The role of nucleotides in vascular calcification has been largely attributed to inorganic pyrophosphate. Genetic studies have shown the important roles for inorganic pyrophosphate (PPi) as inhibitors of vascular mineralization. Deficiency in the mineralization inhibitor PPi, that arises from genetic disruption of the murine ectoezyme NPP1 (ectonucleotide pyrophosphatase/phosphodiesterase I), causes arterial calcification (26). In addition, PPi deficiency due to NPP1 loss-of-function mutations is associated with a rare congenital disorder characterized by generalized arterial calcification in infants (27). The present study identifies an alternative and robust pathway by which extracellular nucleotides acting through P2Y$_2$R inhibit VSMC calcification. Using loss-of-function and gain-of-function experiments, we unequivocally established that P2Y$_2$R is a powerful inhibitor of VSMC calcification. Indeed, we demonstrated that loss of P2Y$_2$R accelerated high phosphate-induced calcium deposition in VSMC. Furthermore, retroviral

transduction of full length wild-type $P2Y_2R$ into $P2Y_2R^{-/-}$ VSMC reduced calcium deposition to levels comparable with those observed in VSMC from WT mice.

Mechanistically, our studies demonstrate that $P2Y_2R$ mediated inhibition of VSMC calcification at least in part through repression of Runx2 transcriptional activity. Runx proteins are targeted to gene regulatory micro-environments within the nucleus, via a specific sub-nuclear targeting signal (44). However, the mechanisms that shuttle Runx2 between the cytoplasm and the nucleus are poorly understood. It was reported that when endogenous Runx2 associates with stabilized microtubules it is held in the cytoplasm and that the Runx2 amino terminus mediates the microtubule association through the alpha/beta tubulin subunits (45) Thus, it is possible that $P2Y_2R$-mediated microtubule/actin organization regulates Runx2 trafficking between the cytoplasm and the nucleus, a process that directly affects Runx2 transcriptional activity.

In conclusion, this study reveals a previously unknown function of $P2Y_2R$ in vascular calcification, which is distinct from deficits in the mineralization inhibitor inorganic pyrophosphate. Our findings provide a new mechanistic insight into the regulation of the osteoblastic trans-differentiation of VSMC by a nucleotide receptor, through Runx2 antagonism. Given that calcification of atherosclerotic lesions is a highly regulated pathological process potentially subject to intervention, $P2Y_2R$ may be targeted for the treatment or prevention of vascular calcification.

Acknowledgments

Financial support

This work was supported by a grant from the National Institutes of Health (1R01HL112883) to Cheikh I. Seye.

Abbreviations

CDK	chronic kidney disease
ENPP1	ectonucleotide pyrophosphatase-phosphodiesterase 1
$P2Y_2R$	$P2Y_2$ nucleotide receptor
Runx2	Runt related transcription factor-2
TRAP	tartrate-resistant acid phosphatase
VCAM-1	vascular cell adhesion molecule-1
SMC	smooth muscle cells

References

1. Block GA. Prevalence and clinical consequences of elevated Ca x P product in hemodialysis patients. Clin Nephrol. 2000; 54:318–324. [PubMed: 11076108]
2. Zhu D, Mackenzie NCW, Farquharson C, et al. Mechanisms and clinical consequences of vascular calcification. Front Endocrinol. 2012; 3:95.

3. Shroff RC, McNair R, Figg N, Skepper JN, Schurgers L, Gupta A, Hiorns M, Donald AE, Deanfield J, Rees L, Shanahan CM. Dialysis accelerates medial vascular calcification in part by triggering smooth muscle cell apoptosis. Circulation. 2008; 118:1748–1757. [PubMed: 18838561]
4. Goodman WG, London G, Amann K, Block GA, Giachelli C, Hruska KA, Ketteler M, Levin A, Massy Z, McCarron DA, Raggi P, Shanahan CM, Yorioka N. Vascular calcification in chronic kidney disease. American journal of kidney diseases. 2004; 43:572–579. [PubMed: 14981617]
5. Moorthi RN, Moe SM. CKD-mineral and bone disorder: core curriculum. Am J KidneyDis. 2011; 58:1022–1036.
6. Guerin AP, Pannier B, Metivier F, Marchais SJ, London GM. Assessment and significance of arterial stiffness in patients with chronic kidney disease. Curr Opin Nephrol Hypertens. 2008; 17:635–641. [PubMed: 19031658]
7. London GM, Guerin AP, Marchais SJ, Metivier F, Pannier B, Adda H. Arterial media calcification in end-stage renal disease: impact on all-cause and cardiovascular mortality. Nephrol Dial Transplant. 2003; 18:1731–1740. [PubMed: 12937218]
8. Kelly RP, Tunin R, Kass DA. Effect of reduced aortic compliance on cardiac efficiency and contractile function of in situ canine left ventricle. Circ Res. 1992; 71:490–502. [PubMed: 1386792]
9. Niederhoffer N, Lartaud-Idjouadiene I, Giummelly P, Duvivier C, Peslin R, Atkinson J. Calcification of medial elastic fibers and aortic elasticity. Hypertension. 1997; 29:999–1006. [PubMed: 9095090]
10. Beadenkopf WG, Daoud AS, Love BM. Calcification in the coronary arteries and its relationship to arteriosclerosis and myocardial infarction. Am J Roentgenol Radium Ther Nucl Med. 1964; 92:865–887.
11. Kelly-Arnold A, Maldonado N, Laudier D, Aikawa E, Cardoso L, Weinbaum S. Revised microcalcification hypothesis for fibrous cap rupture in human coronary arteries. Proc Natl Acad Sci. 2013; 110:10741–10746. [PubMed: 23733926]
12. Ehara S, Kobayashi Y, Yoshiyama M, Shimada K, Shimada Y, Fukuda D, Nakamura Y, Yamashita H, Yamagishi H, Takeuchi K, Naruko T, Haze K, Becker AE, Yoshikawa J, Ueda M. Spotty calcification typifies the culprit plaque in patients with acute myocardial infarction: an intravascular ultrasound study. Circulation. 2004; 110:3424–3429. [PubMed: 15557374]
13. Shroff RC, McNair R, Figg N, et al. Dialysis accelerates medial vascular calcification in part by triggering smooth muscle cell apoptosis. Circulation. 2008; 118:1748–1757. [PubMed: 18838561]
14. Zhu D, Mackenzie NC, Millan JL, et al. The appearance and modulation of osteocyte marker expression during calcification of vascular smooth muscle cells. PloS ONE. 2011; 6:e19595. [PubMed: 21611184]
15. Collin-Osdoby P. Circ Res. 2004; 95:1046–1057. [PubMed: 15564564]
16. Schroeder TM, Jensen ED, Westendorf JJ. Runx2: a master organizer of gene transcription in developing and maturing osteoblasts. Birth Defects Res C Embryo Today. 2005; 75:213–225. [PubMed: 16187316]
17. Komori T, Yagi H, Nomura S, Yamaguchi A, Sasaki K, Deguchi K, Shimizu Y, Bronson RT, Gao YH, Inada M, Sato M, Okamoto R, Kitamura Y, Yoshiki S, Kishimoto T. Targeted disruption of Cbfa1 results in a complete lack of bone formation owing to maturational arrest of osteoblasts. Cell. 1997; 89:755–764. [PubMed: 9182763]
18. Otto F, Thornell AP, Crompton T, Denzel A, Gilmour KC, Rosewell IR, Stamp GW, Beddington RS, Mundlos S, Olsen BR, Selby PB, Owen MJ. Cbfa1, a candidate gene for cleidocranial dysplasia syndrome, is essential for osteoblast differentiation and bone development. Cell. 1997; 89:765–771. [PubMed: 9182764]
19. Ducy P, Zhang R, Geoffroy V, Ridall AL, Karsenty G. Osf2/Cbfa1: atranscriptional activator of osteoblast differentiation. Cell. 1997; 89:747–754. [PubMed: 9182762]
20. Lian JB, Javed A, Zaidi SK, Lengner C, Montecino M, van Wijnen AJ, Stein JL, Stein GS. Regulatory controls for osteoblast growth and differentiation: role of Runx/Cbfa/AML factors. Crit Rev Eukaryot Gene Expr. 2004; 14:1–41. [PubMed: 15104525]
21. Aikawa E, Nahrendorf M, Sosnovik D, Lok VM, Jaffer FA, Aikawa M, Weissleder R. Multimodality Molecular Imaging Identifies Proteolytic and Osteogenic Activities in Early Aortic Valve Disease. Circulation. 2007; 115:377–386. [PubMed: 17224478]

22. Engelse MA, Neele JM, Bronckers AL, Pannekoek H, de Vries CJ. Vascular calcification: expression patterns of the osteoblast-specific gene core binding factor α-1 and the protective factor matrix gla protein in human atherogenesis. Cardiovasc Res. 2001; 52:281–289. [PubMed: 11684076]
23. Tyson KL, Reynolds JL, McNair R, Zhang Q, Weissberg PL, Shanahan CM. Osteo/Chondrocytic Transcription Factors and Their Target Genes Exhibit Distinct Patterns of Expression in Human Arterial Calcification. Arterioscler Thromb Vasc Biol. 2003; 23:489–494. [PubMed: 12615658]
24. Byon CH, Javed A, Dai Q, Kappes JC, Clemens TL, Darley-Usmar VM, McDonald JM, Chen Y. Oxidative stress induces vascular calcification through modulation of the osteogenic transcription factor Runx2 by AKT signaling. J Biol Chem. 2008; 283:15319. [PubMed: 18378684]
25. Sun Y, Byon CH, Yuan K, Chen J, Mao X, Heath JM, Javed A, Zhang K, Anderson PG, Chen Y. Smooth muscle cell-specific runx2 deficiency inhibits vascular calcification. Circ Res. 2012; 111(5):543–52. [PubMed: 22773442]
26. Rutsch F, Ruf N, Vaingankar S, et al. Mutations in ENPP1 are associated with 'idiopathic' infantile arterial calcification. Nat Genet. 2003; 34:379–81. [PubMed: 12881724]
27. St Hilaire C, Ziegler SG, Markello TC, Brusco A, Groden C, Gill F, Carlson-Donohoe H, Lederman RJ, Chen MY, Yang D, Siegenthaler MP, Arduino C, Mancini C, Stanescu HC, Zdebik AA, Chaganti RK, Nussbaum RL, Kleta R, Gahl WA, Boehm M. NT5E Mutations and Arterial Calcifications. N Engl J Med. 2011; 364(5):432–442. [PubMed: 21288095]
28. Prosdocimo DA, Wyler SC, Romani AM, O'Neill WC, Dubyak GA. Regulation of vascular smooth muscle cell calcification by extracellular pyrophosphate homeostasis: synergistic modulation by cyclic AMP and hyperphosphatemia. Am J Physiol Cell Physiol. 2010; 298(3):C702–C713. [PubMed: 20018951]
29. Seye CI, Yu N, Jain R, Kong Q, Minor T, Newton J, Erb L, Gonzalez FA, Weisman GA. The $P2Y_2$ nucleotide receptor mediates UTP-induced vascular cell adhesion molecule-1 expression in coronary artery endothelial cells. J Biol Chem. 2003; 278:24960–24965. [PubMed: 12714597]
30. Seye CI, Yu N, Gonzalez FA, Erb L, Weisman GA. The $P2Y_2$ Nucleotide Receptor Mediates Vascular Cell Adhesion Molecule-1 Expression through Interaction with VEGF Receptor-2 (KDR/Flk-1). J Biol Chem. 2004; 279:35679–35686. [PubMed: 15175347]
31. Seye CI, Kong Q, Erb L, Garrad RC, Krugh B, Wang M, Turner JT, Sturek M, Gonzalez FA, Weisman GA. Functional $P2Y_2$ nucleotide receptors mediate uridine 5′-triphosphate-induced intimal hyperplasia in collared rabbit carotid arteries. Circulation. 2002; 106:2720–2726. [PubMed: 12438299]
32. Qian, Shaomin, Hoggatt, April, Jones-Hall, Yava L., Ware, Carl F., Herring, Paul, Seye, Cheikh I. Deletion of $P2Y_2$ Receptor Reveals a Role for Lymphotoxin-α in Fatty Streak Formation. Vascul Pharmacol. 2016; 85:11–20. [PubMed: 27355755]
33. Van Vlijmen BJ, et al. Diet-induced hyperlipoproteinemia and atherosclerosis in apolipoprotein E3-Leiden transgenic mice. J Clin Invest. 1994; 93:1403–10. [PubMed: 8163645] Westenfeld R, Schäfer C, Smeets R, Brandenburg VM, Floege J, Ketteler M, Jahnen-Dechent W. Fetuin-A (AHSG) prevents extraosseous calcification induced by uraemia and phosphate challenge in mice. Nephrol Dial Transplant. 2007; 22(6):1537–46. [PubMed: 17389622]
34. Feng B, Zhang D, Kuriakose G, Devlin CM, Kockx M, Tabas I, Niemann-Pick C. Heterozygosity confers resistance to lesional necrosis and macrophage apoptosis in murine atherosclerosis. Proc Natl Acad Sci U S A. 2003; 100:10423–10428. [PubMed: 12923293]
35. Yu N, Erb L, Shivaji R, Weisman GA, Seye CI. Binding of the P2Y2 nucleotide receptor to filamin A regulates migration of vascular smooth muscle cells. Circ Res. 2008; 102:581–588. [PubMed: 18202316]
36. Seye CI, Agca Y, Agca C, Derbigny W. $P2Y_2$ receptor-mediated lymphotoxin-α (LTA) secretion regulates intercellular cell adhesion molecule (ICAM)-1 expression in vascular smooth muscle cells. J Biol Chem. 2012; 287:10535–10543. [PubMed: 22298782]
37. Rattazzi M, Bennett BJ, Bea F, Kirk EA, Ricks JL, Speer M, Schwartz SM, Giachelli CM, Rosenfeld ME. Calcification of advanced atherosclerotic lesions in the innominate arteries of ApoE-deficient mice: potential role of chondrocyte-like cells. Arterioscler Thromb Vasc Biol. 2005; 25:1420–1425. [PubMed: 15845913]

38. Speer MY, Chien YC, Quan M, Yang HY, Vali H, McKee MD, Giachelli CM. Smooth muscle cells deficient in osteopontin have enhanced susceptibility to calcification in vitro. Cardiovasc Res. 2005; 66(2):324–33. [PubMed: 15820201]

39. Lin ME, Chen T, Leaf EM, Speer MY, Giachelli CM. Runx2 Expression in Smooth Muscle Cells Is Required for Arterial Medial Calcification in Mice. Am J Pathol. 2015; 185(7):1958–1969. [PubMed: 25987250]

40. Zhang H, Pan Y, Zheng L, Choe C, Lindgren B, Jensen ED, Westendorf JJ, Cheng L, Huang H. FOXO1 inhibits Runx2 transcriptional activity and prostate cancer cell migration and invasion. Cancer Res. 2011; 71(9):3257–3267. [PubMed: 21505104]

41. Elliott MR, Chekeni FB, Trampont PC, Lazarowski ER, Kadl A, Walk SF, Park D, Woodson RI, Ostankovich M, Sharma P, Lysiak JJ, Harden TK, Leitinger N, Ravichandran KS. Nucleotides released by apoptotic cells act as a find me signal to promote phagocytic clearanc. Nature. 2009; 461(7261):282–286. [PubMed: 19741708]

42. Achenbach S, Ropers D, Pohle K, Leber A, Thilo C, Knez A, Menendez T, Maeffert R, Kusus M, Regenfus M, Bickel A, Haberl R, Steinbeck G, Moshage W, Daniel WG. Influence of lipid-lowering therapy on the progression of coronary artery calcification: a prospective evaluation. Circulation. 2002; 106(9):1077–1082. [PubMed: 12196332]

43. Pugliese G, Iacobini C, Blasetti Fantauzzi C, Menini S. The dark and bright side of atherosclerotic calcification. Atherosclerosis. 2015; 238(2):220–30. [PubMed: 25528431]

44. Zaidi, Sayyed K., Young, Daniel W., Choi, Je-Yong, Pratap, Jitesh, Javed, Amjad, Montecino, Martin, Stein, Janet L., van Wijnen, Andre J., Lian, Jane B., Stein, Gary S. The dynamic organization of gene-regulatory machinery in nuclear microenvironments. EMBO Rep. 2005; 6(2): 128–133. [PubMed: 15689940]

45. D'Addario M, Arora PD, Ellen RP, McCulloch CA. Regulation of tension-induced mechanotranscriptional signals by the microtubule network in fibroblasts. J Biol Chem. 2003; 278(52):53090–53097. [PubMed: 14561736]

46. Pockwinse SM, Rajgopal A, Young DW, Mujeeb KA, Nickerson J, Javed A, Redick S, Lian JB, van Wijnen AJ, Stein JL, Stein GS, Doxsey SJ. Microtubule-dependent nuclear-cytoplasmic shuttling of Runx2. J Cell Physiol. 2006; 206(2):354–362. [PubMed: 16110492]

Highlights

- $P2Y_2$ receptor deficiency in *ApoE*$^{-/-}$ mice reduces atherosclerosis
- Loss of $P2Y_2$ receptor accelerates arterial intimal calcification in *ApoE*$^{-/-}$ mice
- Expression of $P2Y_2$ receptor inhibits high phosphate-induced smooth muscle cell calcification
- $P2Y_2$ receptor negatively regulates Runx2 transcriptional activity in smooth muscle cells.

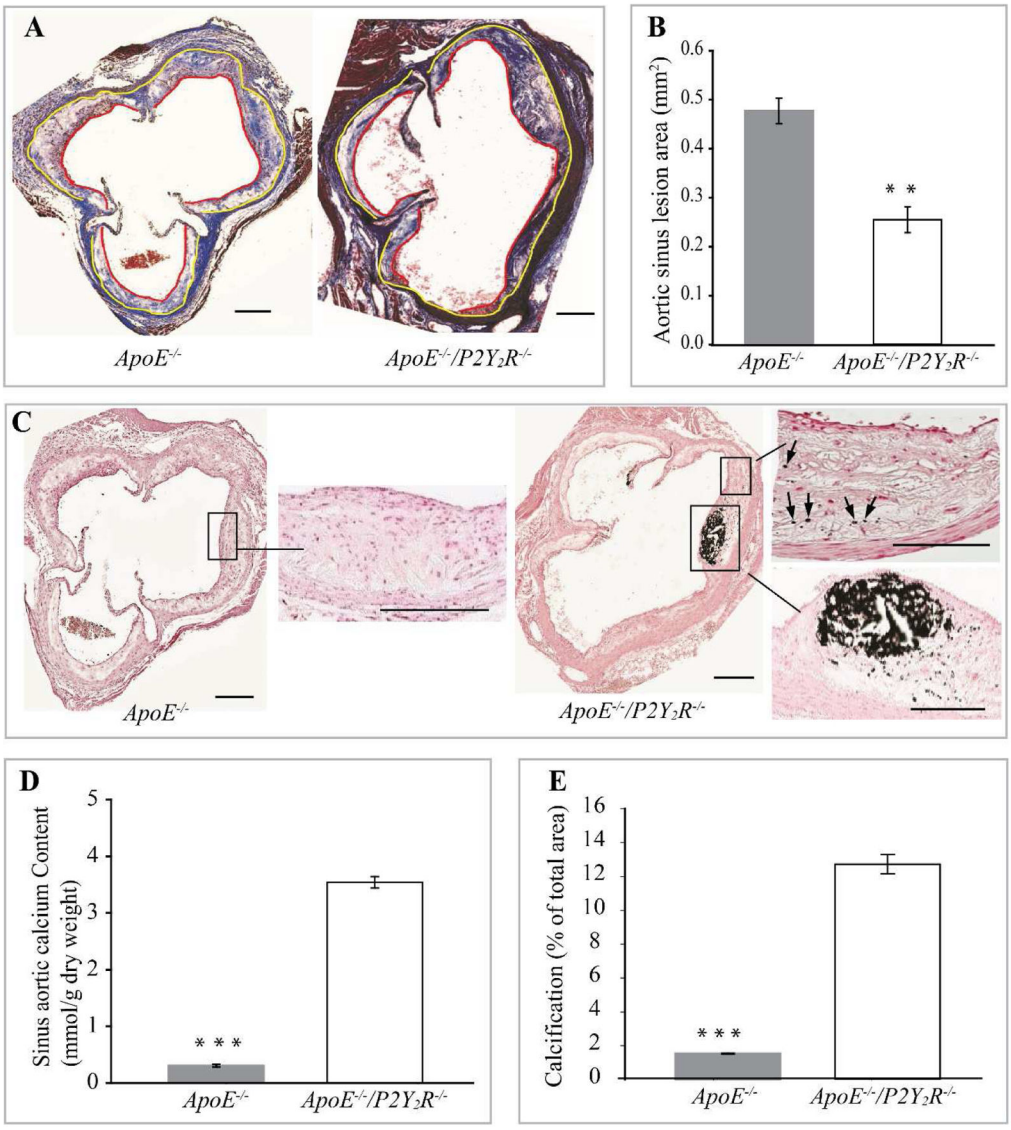

Fig. 1. $P2Y_2$ receptor deficiency reduces atherosclerosis and increases calcification of atherosclerotic lesions

(A) Light micrographs of representative Masson's trichrome stained aortic root lesions from *ApoE*$^{-/-}$ and *ApoE*$^{-/-}$/*P2Y*$_2$*R*$^{-/-}$ mice, showing atherosclerotic lesion (area between yellow and red lines) as well as collagen and muscle fibers in the lesions. (B) Quantitative analysis of lesions in the aortic sinus. Data represent the mean ± SEM lesion area for 5 consecutive sections in each of the 12 mice examined for each genotype. (*p<0.001). Scale represents 100 μm. Arrows indicate lesions. (C) Representative images of sections stained with Von Kossa to detect calcification. Areas in insert have been magnified. Arrows indicate spotty calcium deposits. Scale bar = 100μm. (D) Quantification of the sinus aortic calcium content expressed as mmol/g of dried weight and (E) calcification presented as percentage of Von Kossa-positively stained areas in the total aortic lesion. Quantification was done using 5 cross sections in each of the 12 *ApoE*$^{-/-}$ mice and 12 *ApoE*$^{-/-}$/*P2Y*$_2$*R*$^{-/-}$ mice. Bar values are means ± SEM, *p<0.001.

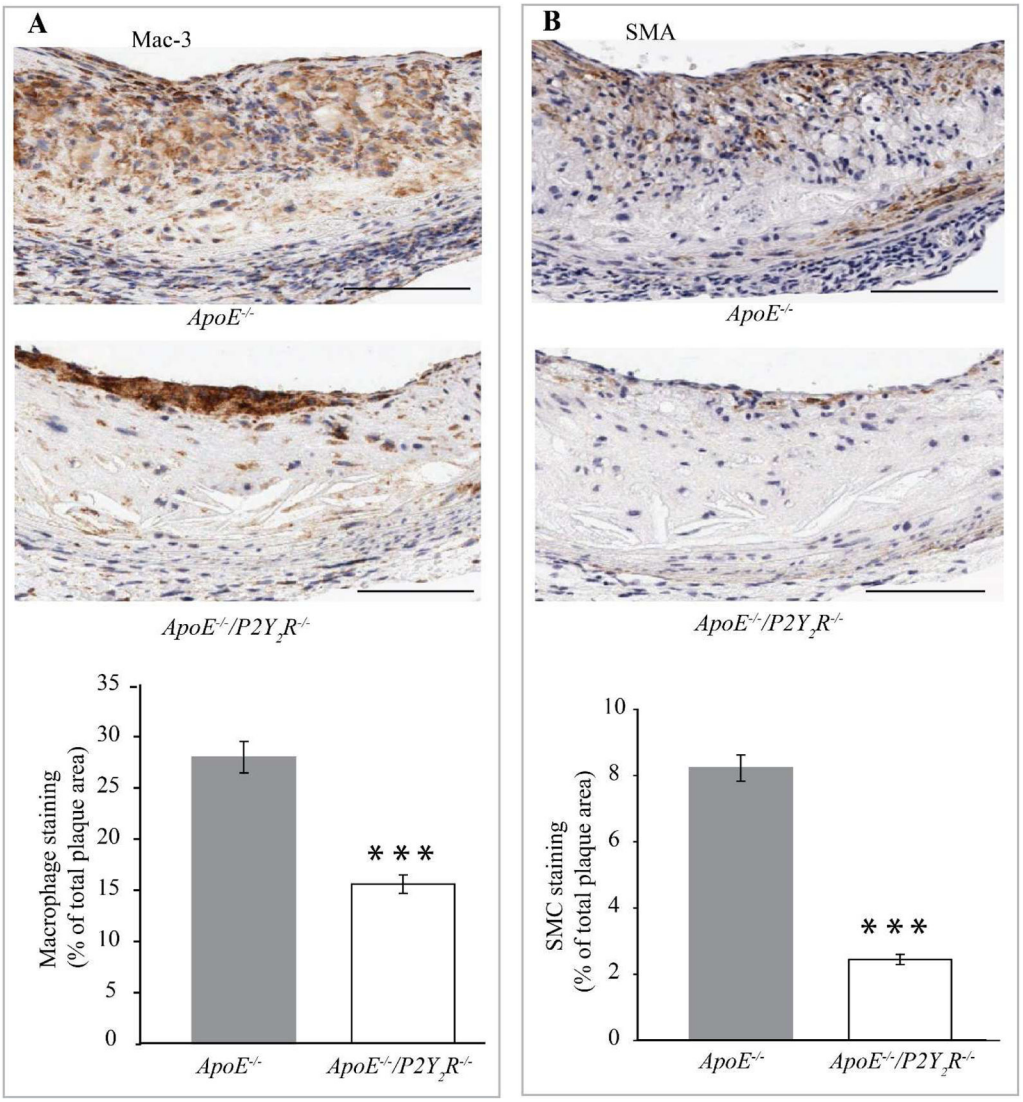

Fig. 2. P2Y$_2$ receptor modulates cellular composition and cellularity of atherosclerotic lesions

(A and B) Representative images of immunohistological staining of atherosclerotic lesions in the aortic sinus. Adjacent sections were stained with (A) Mac-3 or (B) smooth muscle α-actin antibodies, respectively. The percentage of Mac-3 or smooth muscle α-actin-positive areas in A and B was calculated by dividing the positively stained areas by the total cross-sectional area of the lesion. Bar values are means ± SEM. Five cross sections were evaluated in 12 mice for each genotype. ***p<0.001. Arrows indicate the localization of the staining. Scale bar represents 100 μm.

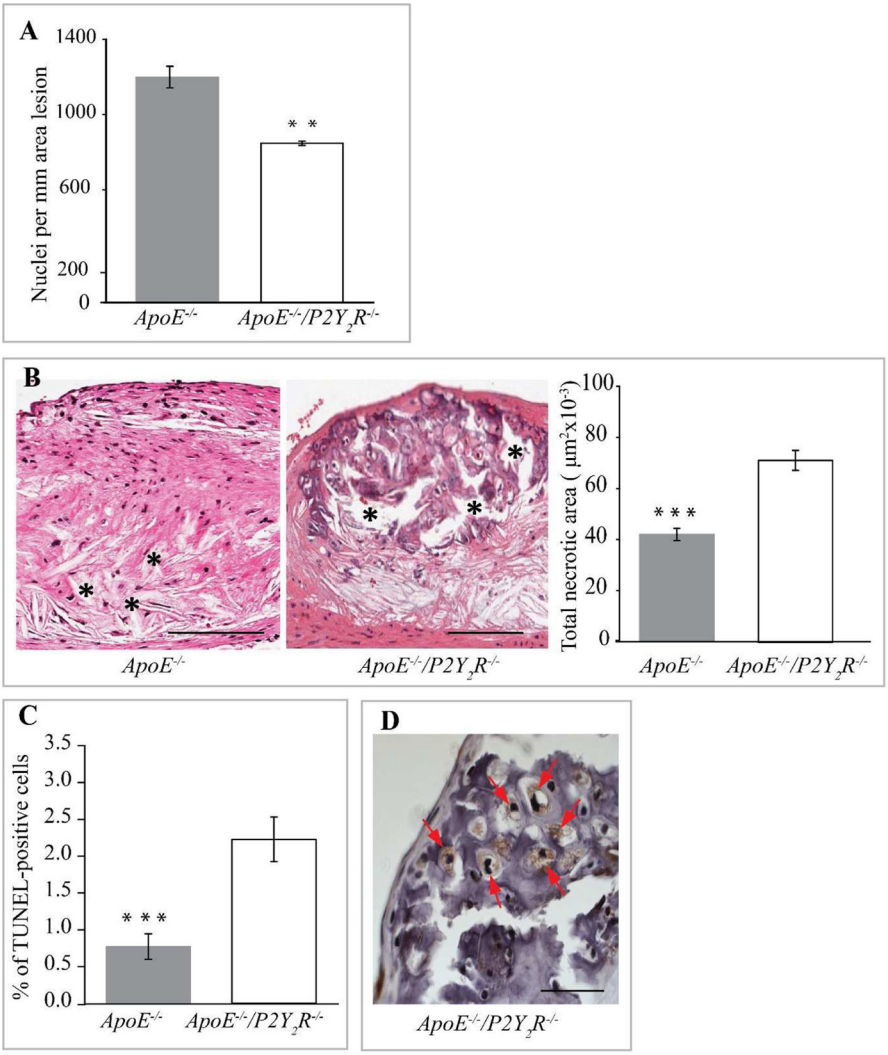

Fig. 3. Reduction of plaque cellularity in *ApoE*$^{-/-}$/*P2Y*$_2$*R*$^{-/-}$ mice

(A) Total nuclei were counted in each hematoxylin eosin-stained cross sections (n=5) from 12 mice in each group and normalized to the area lesion. **p<0.01. Scale bar represents 100 µm. (B) Evaluation of plaque necrosis. Representative images of aortic root sections (n=5) from 12 mice of each group genotype were stained with hematoxylin and eosin, and plaque necrosis was quantified. Necrotic areas are indicated with an asterisk. ***p<0.001. Scale bar represents 100 µm. (C) TUNEL-positive nuclei were quantified on lesions from 12 *ApoE*$^{-/-}$ and 13 *ApoE*$^{-/-}$/*P2Y*$_2$*R*$^{-/-}$ mice.***p<0.001. (D) High magnification of aortic root cross section from *ApoE*$^{-/-}$/*P2Y*$_2$*R*$^{-/-}$ mice showing chondrocyte-like cells (asterisk) within large areas of calcification. Scale bar represents 25 µm.

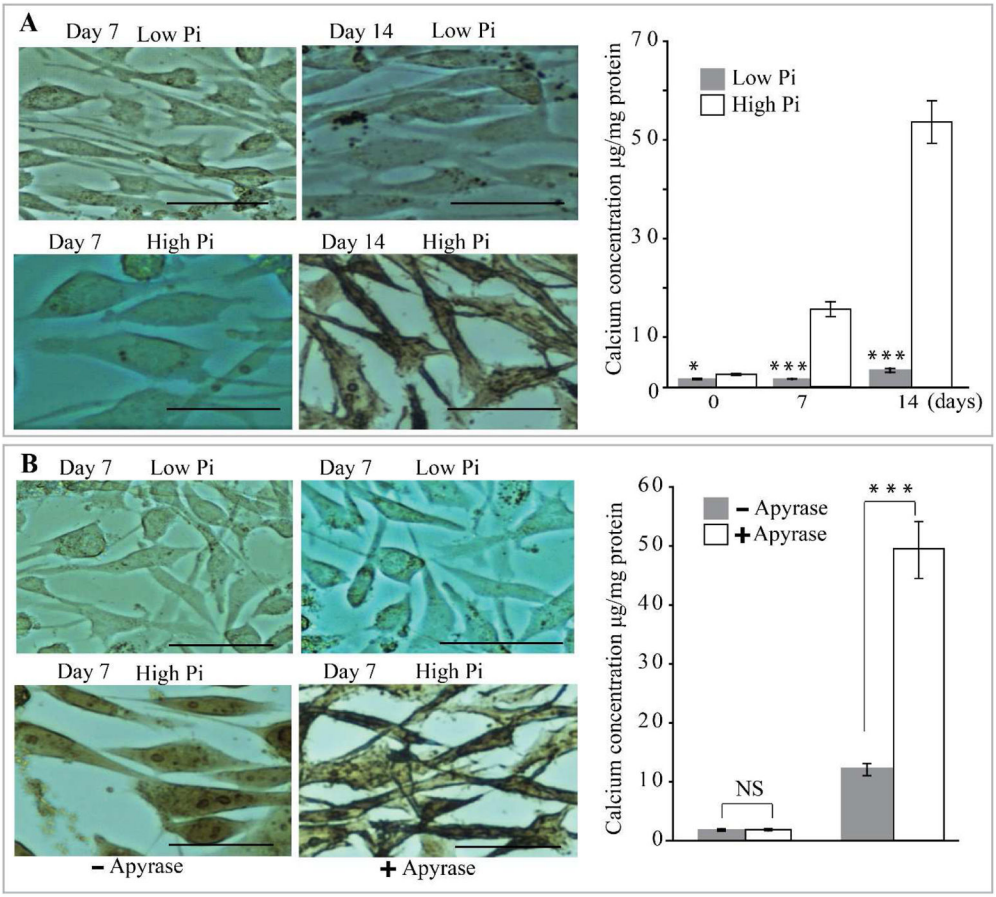

Fig. 4. P2Y$_2$R deficiency in VSMC enhances high phosphate-induced calcification in VSMC

(A) Wild-type (WT) and *P2Y$_2$R*$^{-/-}$ VSMC were incubated in high phosphate (High Pi) or control medium (Low Pi) for 7 or 14 days and stained with alizarin red. Calcium deposition was quantified. Results are presented as mean ± SEM. *p<0. 05; ***p < 0.001; n=4 independent experiments. (B) VSMC were cultured in high or low phosphate medium in the absence or presence of apyrase. Calcium deposition was quantified as in (A). Data represent mean ± SEM of 5 independent experiments. NS= Not significant; ***p < 0.001. Scale bar =100 µm.

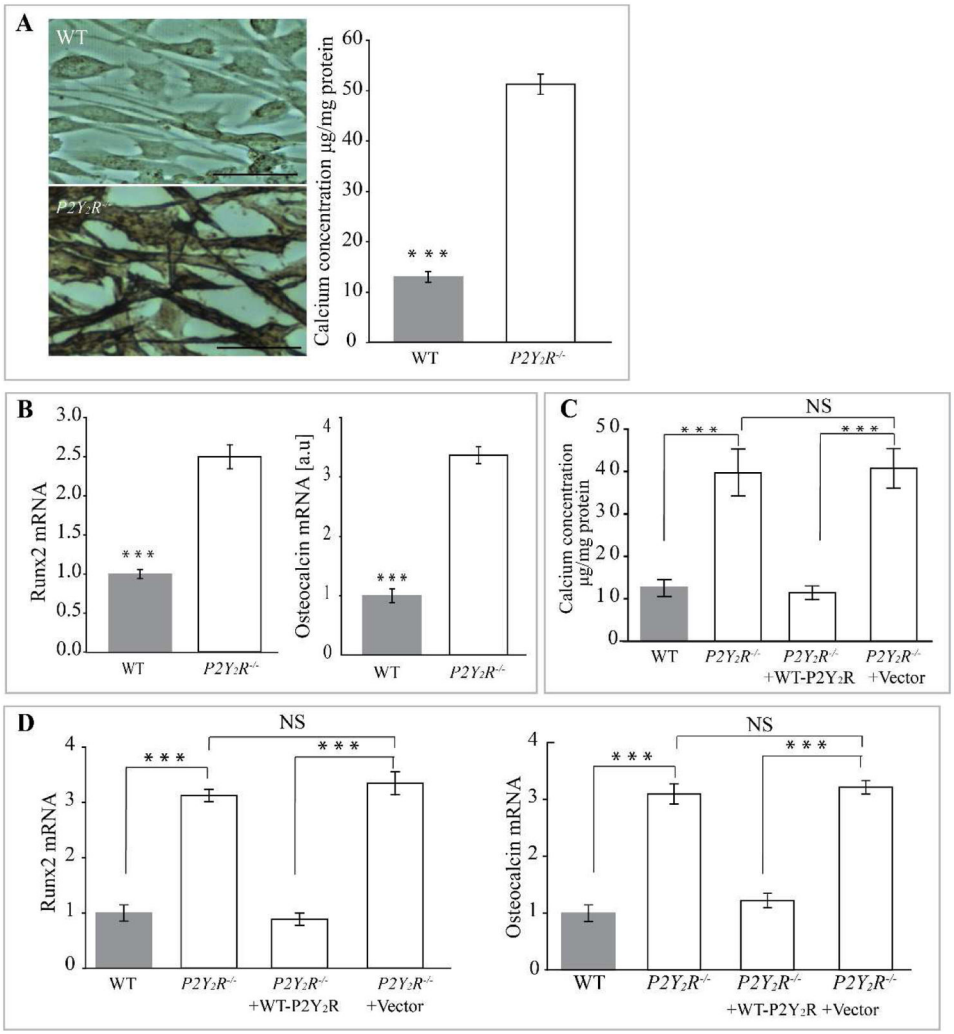

Fig. 5. Expression of $P2Y_2$ receptor prevents smooth muscle cell calcification *in vitro*

(A) Wild-type (WT) and $P2Y_2R^{-/-}$ VSMC were incubated in high phosphate (High Pi) or control medium (Low Pi) for 7 days and stained with alizarin red. Scale bar =100µm. (B) Calcium deposition in VSMC was quantified as in Fig. 4. Fold changes in the mRNA expression of osteogenic markers Runx2 and osteocalcin relative to that seen in WT cells are shown in bar graphs. Results are presented as mean ± SEM. ***$p < 0.001$; n=4 independent experiments. Transduction of WT $P2Y_2R$ into $P2Y_2R^{-/-}$ inhibits (C) calcium deposition as well as (D) relative mRNA levels for Runx2 and osteocalcin. ***$p < 0.001$; n=3 independent experiments; NS= not significant.

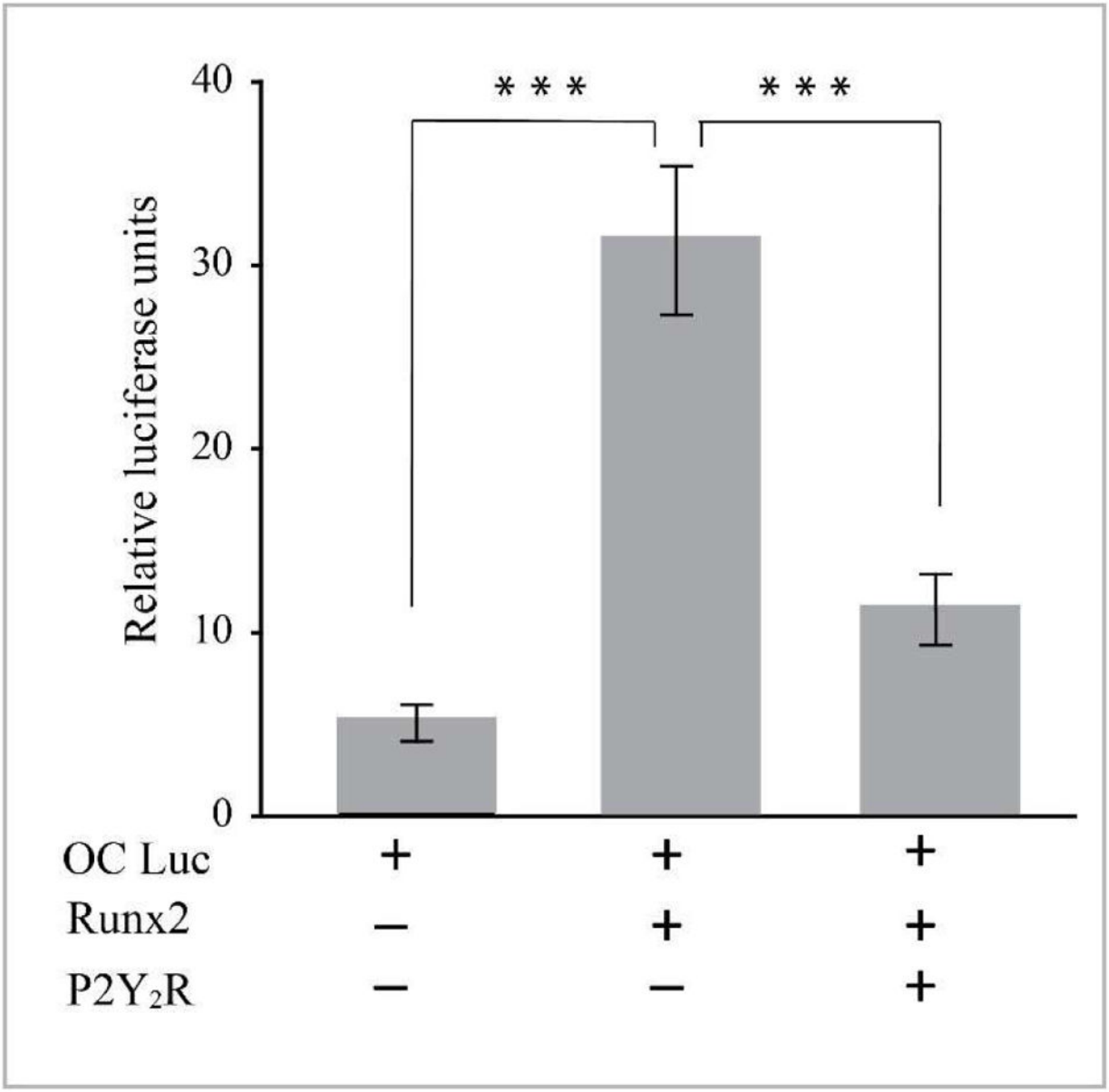

Fig. 6. P2Y$_2$R inhibits Runx2-activation of the osteocalcin promoter

P2Y$_2$R-null VSMC were transfected with an osteocalcin promoter luciferase reporter gene, an internal control pRL-TK plasmid, a Runx2 expression plasmid, and a full length P2Y$_2$R expression plasmid as indicated. Lysates were harvested 48 h after transfection and were normalized to the expression of the pRL-TK plasmid. Results are presented as the mean ± SD of triplicates of cells and are representative of three independent experiments. ***p<0.001.

Table 1

Body weight and plasma lipid analysis in standard chow-fed *ApoE*$^{-/-}$ and *ApoE*$^{-/-}$/*P2Y*$_2$*R*$^{-/-}$ mice.

Week 30 (n=11)	***ApoE*$^{-/-}$**	***ApoE*$^{-/-}$/*P2Y*$_2$*R*$^{-/-}$**
Body weight (g)	37.2.5 ± 2	36 ± 1.8
Total cholesterol (mg/dl)	459 ± 35	452 ± 29
Triglycerides (md/dl)	74 ± 9	76 ± 7